RSC Advances

ROYAL SOCIETY OF CHEMISTRY

www.rsc.org/advances

Cite this: DOI: 10.1039/c0xx00000x

www.rsc.org/xxxxxx

ARTICLE

Water-dispersible and stable fluorescent Maya Blue-like pigments

Yujie Zhang,[a, b] Ling Fan,[a, c] Junping Zhang,*[a, c] and Aiqin Wang*[a, c]

Received (in XXX, XXX) Xth XXXXXXXXX 20XX, Accepted Xth XXXXXXXXX 20XX
DOI: 10.1039/b000000x

Poor water-dispersibility and stability of hydrophobic fluorescent organic pigments (HFOPs) hinder many of their applications. Inspired by the excellent stability of Maya Blue pigments and the water solubility of Laponite RD (LRD), we report facile synthesis of water-dispersible and stable fluorescent Maya Blue-like pigments via the host-guest interaction between LRD and Pigment Red 31 (PR 31), a representative HFOP. The concentration of LRD and solid-state grinding play important roles in effectively dispersing PR 31 into the aqueous solution. The interactions between PR 31 and LRD involve van der Waals, π-π, electrostatic, hydrogen bonding between phenolic hydroxyl groups of PR 31 and silanols of LRD as well as dye-dye hydrophobic interactions. The interactions between PR 31 and LRD occur on the external surface of LRD and the entrance of the micropores of LRD, however, the PR 31 molecules cannot intercalate into the layers of LRD plates. The so-obtained pigments are highly water-dispersible, and very stable to thermal aging and UV irradiation owing to the interactions between LRD and PR 31, and the shielding effect of LRD.

Introduction

The low dispersibility or solubility of hydrophobic organic compounds in the aqueous phase is the common problem in chemical experiments and industry. Bringing these hydrophobic compounds into aqueous solutions is of general interests for the scientific community and the industrial area. Hydrophobic fluorescent organic pigments (HFOPs) have attracted much attention in diverse fields, e.g., coatings, inks and plastics, owing to their bright color and light tone.[1] However, HFOPs tend to agglomerate in aqueous phase due to the big difference in polarity between pigments and water. Consequently, HFOPs cannot be used in aqueous solutions and harmful organic solvents must be employed to dissolve or disperse them. Also, the thermal stability and photostability of HFOPs remain to be improved. Thus, preparation of water-dispersible and stable HFOPs is a major challenge but a prerequisite for many of their potential applications.

Generally, the methods developed so far to improve the water-dispersibility and stability of organic pigments can be categorized into (1) chemical derivatization,[2] (2) incorporation in polymer matrices,[3] (3) incorporation in inorganic oxides (such as SiO_2, TiO_2 and Al_2O_3),[4, 5] and (4) solubilization in non-conventional media (e.g., supercritical CO_2 and surfactants).[6] Nevertheless, these procedures can hardly be deemed flawless. The chemical derivatization requires specific reagent for each pigment family and inconvenient purification, impeding its universality.[7] The incorporation methods, regardless of organic or inorganic, suffer tedious experimental process, especially in the case of layer-by-layer assembly, but often offer uncontrollable results. More specifically, the process of coating pigments with silica has certain inevitable demerits, such as low surface deposition content and intractable reproducibility.[8] In view of the above issues, it would be of immense interest if the water-dispersibility and stability of HFOPs could be enhanced remarkably while minimizing the impacts by these drawbacks.

Maya Blue, a palygorskite/indigo hybrid, is a well-known artificial pigment widely used by ancient Mayan in Yucatan.[9-14] The astonishing stabilities of Maya Blue against acid, alkali and various solvents have fascinated numerous chemists, material scientists and archaeologists. The hydrogen bonding between indigo and palygorskite was widely agreed to be responsible for the unusual stability of Maya Blue. The proposed hydrogen bonding hypothesis include: (1) carbonyl and amino of indigo with edge silanols of palygorskite,[15] (2) carbonyl of indigo with structural water inside the micro-channels of palygorskite,[16-19] and (3) carbonyl of indigo with structural water accompanied by direct interaction between indigo and octahedral cations of palygorskite as well as Van der Waals interaction.[16] There is also a viewpoint that different types of interactions are present in the structure of Maya Blue.[20] In addition, for some researchers, the stability of Maya Blue depends more on steric shielding than on hydrogen bonding.[21] The definite position of indigo molecules in the palygorskite is still in dispute. Some are of opinion that the indigo molecules occupy the channels of palygorskite after thermal treatment, which was previously filled with water molecules.[22, 23] Whereas some believe that the indigo molecules only block the entrance of the channels, rather than reside in the channel.[24] Although the real recipe of Mayan to prepare Maya Blue is unknown, grinding and heating the mixture of palygorskite and indigo is the most frequently employed strategy thus far to promote the interaction between them.[25, 26]

Inspired by the excellent stability of Maya Blue and the water solubility of Laponite RD (LRD), here we report facile preparation of water-dispersible and stable Maya Blue-like pigments composed of a clay mineral, LRD, and Pigment Red 31 (PR 31). LRD, $Na_{0.7}[Mg_{5.5}Li_{0.3}Si_8O_{20}(OH)_4](H_2O)_n$, is a synthetic hectorite-type clay mineral consisting of monodispersed and well defined platelets with a diameter of 25~30 nm and a thickness of approximately 1 nm, and a negative surface charge density of 0.014 $e^-/Å^2$.[27] Different from most of the other clay minerals, LRD is soluble in aqueous solution at concentration below 5 wt% with negative face charges and positive edge charges on the platelets.[28] PR 31, a fluorescent azo-pigment, is widely used for the coloration of rubber, fabric, paints, plastics and printing ink. PR 31 is one of the oldest commercially available magenta pigments. However, the hydrophobicity and the low thermal- and photo-stability hinder many of its applications as mentioned in the introduction. Thus, PR 31 was chosen as the representative HFOP in this study. LRD could successfully bring indigo, the main organic component in Maya Blue, into the aqueous phases according to Lezhnina et al.[29] Whereas the marriage between LRD and PR 31 via solid-state grinding generates not only water-dispersible but also stable fluorescent pigments, which we term Maya-Blue like LRD/PR 31 pigments. The representative LRD/PR 31 pigment is highly water-dispersible after ultrasonication and the concentration of PR 31 in water is as high as 9.97 mg/mL which is much higher than the LRD/indigo dispersion (0.2 mg/mL) produced by Lezhninaet al.[29] The LRD/PR 31aqueous suspension shows excellent fluorescence and is stable in room conditions for over 4 months without any sediment. The concentration of LRD and grinding time play important roles in bringing PR 31 into aqueous suspensions. Moreover, LRD/PR 31 is very stable to thermal aging and UV irradiation in comparison with pristine PR 31 owing to the interactions between LRD and PR 31 as well as the shielding effect of LRD.

Experimental section

Materials

PR 31 (3-hydroxy-4-[[2-methoxy-5-[(phenylamino)carhonyl]phenyl]azo]-*N*-(3-nitrophenyl)-2-naphthalenecarboxamide) was purchased from Liwang Chemical Co., Ltd. (China). PR 31 was used after washing 3 times by ethanol in order to remove the impurity. LRD was supplied by Southern Clay Products, Inc. Deionized water was used for preparing the LRD/PR 31 aqueous suspensions. Other reagents used were all of analytical grade.

Preparation of LRD/PR 31 aqueous suspensions

The LRD/PR 31 hybrid pigments were prepared according to the following procedure. 200 mg of LRD powder was mixed with a given dosage of PR 31 and hand-ground for a predetermined time to form a homogeneous rose-red mixture. During grinding, the powder adhered to the surface of mortar and pestle. The powder was scraped off with a spatula and ground again. The process was repeated several times until a homogeneous powder was formed.

Preparation of LRD/PR 31 aqueous suspensions was carried out as follows. Typically, the fine powder was dispersed into a given amount of deionized water in a vial and stirred magnetically for 3 min followed by ultrasonication for 30 min at 25°C. The LRD/PR 31 suspension was then obtained after centrifugating the mixture at 8000 rpm for 20 min to remove the aggregates. Suspensions for further analyses were prepared by diluting the original suspension with deionized water.

Measurement of PR 31 concentration in aqueous dispersions

To evaluate and compare the concentration of PR 31 in the aqueous phase, the suspensions were analyzed by measuring the absorbance at 568 nm using a UV-Vis spectrophotometer (Specord 200, Analytik Jena AG). Deionized water was used as the blank. The relationship between the concentration of PR 31 in the aqueous phase and the absorbance at 568 nm can be seen from the standard curve (Fig. S1).

Stability tests

In order to compare thermal stability differences between PR 31 and LRD/PR 31, specimens were placed in an oven at 150 °C for 4 h. Photostability of samples was carried out in a UV Accelerated Weathering Tester (ZN-P, Xinlang, Shanghai, China) with eight UV-B (280 ~ 315 nm) tubes (40 w) for 48 h. The intensity of radiation is 0.6w/m^2. The temperature was maintained at 60°C during UV irradiation. 0.3 g of sample was dispersed in 40 mL of acetone followed by spray-coating on an aluminium plate and drying at room temperature. Then the samples on aluminum plates were placed in the UV Accelerated Weathering Tester.

Characterization

The micrographs of the samples were taken using a field emission transmission electron microscope (TEM, JEM-1200EX, FEI). A drop of the LRD/PR 31 aqueous suspension (diluted 20-fold) was put on a copper microgrid and dried in the open atmosphere. The elemental maps of C and Si in the LRD/PR 31 pigment were obtained using an energy dispersive spectrometer (EDS) attached to TEM. SEM observation of LRD/PR 31 was carried out using scanning electron microscopy (JSM-6701F, JEOL, Ltd) after coated by a gold film. Water contact angles and a high speed video (400 fps) were taken using the Contact Angle System OCA 20, Dataphysics (Germany). The zeta potentials of the samples were measured by Zetasizer Nano ZS (Malvern Instruments Ltd., Worcestershire, UK). FTIR spectra of samples were collected on a Thermo Nicolet NEXUS TM spectrophotometer (Thermo, Madison, USA) in the range of 4000-400 cm^{-1} using KBr pellets. The pore volume and surface area of the samples were determined by N_2 sorption isotherm and application of the BET theory. The instrument used was a micromeritics ASAP 2020 and the supplied software was used to manipulate the experimental data. Viscosity of the samples was measured using an Anton PaarPhysica MCR301 Rheometer (Germany) with the steady shear rate in the range of 0.1 to 200 s^{-1}. XRD patterns were obtained on X'pert PRO diffractometer with working conditions Cu Kα, 30 mA and 40 kV (λ = 1.54060 Å). The scanning was made at room temperature between 3 and 50º in 2θ with a scanning speed of 0.02º per second. Thermogravimetric analyses (TGA) of samples were carried out on a STA 6000 (Perkin Elmer Instrument Co., Ltd. USA) to investigate the thermal stability of the samples. The temperature program was 10.0 K/min from 20 to 900 °C under N_2 atmosphere.

Results and discussion

Preparation of LRD/PR 31

The LRD/PR 31 pigments were prepared simply by grinding the mixture of LRD and PR 31 powders with an appropriate ratio in an agate mortar for a period of time (Fig. 1a). Solid-state grinding is a very important procedure for preparing Maya Blue and other functional materials by promoting the interactions between guest and host species.[30, 31] The mixture of white LRD and rose-red PR 31 became a homogeneous rose-red powder after ground for a few minutes. Such a color change implies interaction between LRD and PR 31. PR 31 is not normally encountered in aqueous solution and is in the form of aggregate once dropped in water because PR 31 is hydrophobic (Fig. 1b). A water drop is spherical in shape with a contact angle of 137º on the surface of the glass slide spray-coated with PR 31 (Fig. 2a, b and Movie S1). However, hand-grinding of PR 31 in the presence of LRD could surprisingly bring hydrophobic PR 31 into aqueous phase (Fig. 1c). This is because LRD/PR 31 is hydrophilic and the water contact angle on the surface of spray-coated LRD/PR 31 is 0º (Fig. 2c, d and Movie S1). Moreover, stable aqueous suspension of LRD/PR 31 can be easily formed by stirring and ultrasonication in deionized water. Once encountered with water, the stacked platelets of LRD/PR 31 automatically exfoliate into individual platelets via electrostatic repulsion to form a network structure.[32, 33] The subsequent ultrasonication helps to disintegrate the agglomerated LRD/PR 31 formed during grinding, and then further increases the concentration of PR 31. The LRD/PR 31 aqueous suspension is very homogeneous and no aggregate of PR 31 was detected (Fig. 1c). The interactions between PR 31 and LRD together with the excellent solubility of LRD in water should be responsible for the transportation of PR 31 into aqueous phase. LRD/PR 31 is in the form of microparticles 0.2 ~ 3 μm in size (Fig. 1d). The TEM image and EDS elemental maps of Si and C of LRD/PR 31 (Fig. 1e-g) demonstrate the uniform distribution of PR 31 in the hybrid pigment.

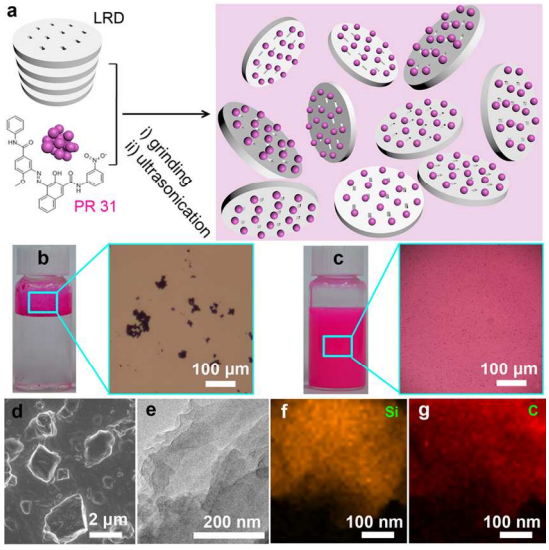

Fig. 1. (a) Schematic illustration for preparing the water-dispersible stable LRD/PR 31 pigment, digital images and optical micrographs of aqueous suspensions of (b) pristine PR 31 and (c) LRD/PR 31 (3.75 mg/mL PR 31), (d) SEM image, (e) TEM image, and (f, g) EDS elemental maps of Si and C of (c).

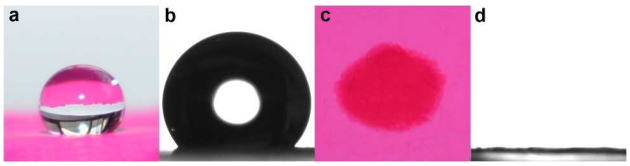

Fig. 2. Digital images of water drops on the powders of (a) PR 31 and (c) LRD/PR 31 and water contact angles of (b) PR 31 and (d) LRD/PR 31. The mixture of 40 mg of PR 31 and 200 mg of LRD was ground for 10 min.

The zeta potential of LRD is -48.37 mV (Table 1) indicating a negatively charged surface of LRD and much better dispersibility of LRD in water compared with palygorskite, whose zeta potential is -17.5 mV.[34] The zeta potential of PR 31 is -2.09 mV, which is consistent with its low dispersibility in water. LRD/PR 31 shows an even lower zeta potential (-55.17 mV) compared with LRD, indicating excellent dispersibility of the LRD/PR 31 pigment in water. The host-guest interaction between LRD and PR 31 should be responsible for the lower zeta potential of LRD/PR 31 since solid-state grinding has no obvious influence on the zeta potential of LRD (Table S1). LRD is capable of adsorbing neutral organic molecules and eventually transport them into aqueous solution,[29] due to the multiple interactions between LRD and organic molecules, such as van der Walls, π-π and electrostatic interactions.[28, 35] It is therefore conceivable that the same mechanisms would influence the interaction between LRD and PR 31 in addition to the hydrogen bonding between phenolic hydroxyl groups of PR 31 and silanols of LRD.

Table 1. Zeta potentials of LRD, PR 31 and LRD/PR 31. The mixture of 40 mg of PR 31 and 200 mg of LRD was ground for 10 min.

Samples	LRD	PR 31	LRD/PR 31
Zeta potentials/ mV	-46.97	-2.09	-55.17

Table 2. BET data of LRD and LRD/PR 31. The mixture of 40 mg of PR 31 and 200 mg of LRD was ground for 10 min.

Samples	S_{BET}(m^2/g)	S_{micro}(m^2/g)	S_{ext}(m^2/g)	V_{total}(cm^3/g)
LRD	325.45	82.51	242.94	0.24
LRD/PR 31	211.04	57.91	153.13	0.17

The FTIR spectra of LRD, PR 31 and LRD/PR 31 shown in Fig. 3 confirm these interactions between LRD and PR 31 again since the band of LRD shifts from 3682 cm^{-1} (stretching vibration of MgO-H) to 3674 cm^{-1} which is consistent with a previous study.[27] The bathochromic shift of LRD from 3449 cm^{-1} (stretching vibration of Si-OH) to 3441 cm^{-1} for LRD supports the proposed hydrogen bonding mechanism. In addition, the dye-dye hydrophobic interaction should also contribute to the dispersion of PR 31 into aqueous solutions.[36] The interaction between PR 31 and LRD also results in decrease in the S_{BET} of LRD by 35% (29.81% of S_{micro} and 36.97% of S_{ext}) when the weight ratio of PR 31 to LRD is 1:5 (Table 2). Meanwhile, the pore volume decreases from 0.24 to 0.17 cm^3/g. In addition, no change of the characteristic diffraction peaks of LRD in the XRD patterns (Fig. S2) can be observed after the introduction of PR 31. This means the crystalline structure of LRD is well preserved and PR 31 molecules did not intercalate into the layers of LRD plates. Thus, the evident decreases in S_{BET} and V_{total} are attributed to blocking of the micropores of LRD by PR 31 molecules and the

host-guest interactions between PR 31 and LRD on the external surface of LRD.

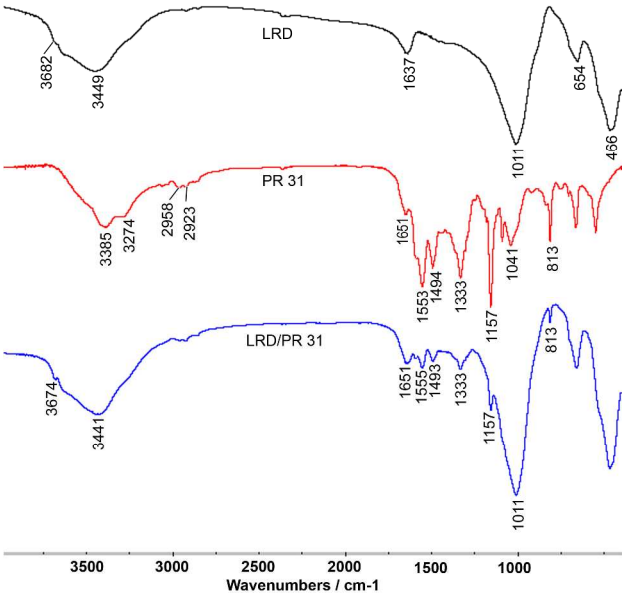

Fig. 3. FTIR spectra of LRD, PR 31 and LRD/PR 31 hybrid. The mixture of 40 mg of PR 31 and 200 mg of LRD was ground for 10 min.

Effects of various parameters on dispersibility and viscosity of LRD/PR 31

The effects of concentration of LRD, dosage of PR 31 and grinding time on concentration of PR 31 in water, percentage of dispersed PR 31 and viscosity of the suspensions are shown in Fig. 4. It is the excellent water solubility of LRD, and the interactions between LRD and PR 31 that successfully bring PR 31 into the aqueous phase. Thus, the dispersibility of PR 31 is significantly influenced by the concentration of LRD as shown in Fig. 4a. The concentration of PR 31 in the aqueous phase was determined via its absorbance at 568 nm using a UV-Vis spectrophotometer (Fig. S1). A critical concentration of 20 mg/mL LRD is necessary to effectively (>90%) disperse PR 31 in deionized water. Below the critical concentration, both the concentration and percentage of dispersed PR 31 in water are very low. The concentration of PR 31 suddenly increases to 3.75 mg/mL with increasing the LRD concentration to 20 mg/mL and over 90% of PR 31 is successfully dispersed in water. The viscosity of the LRD/PR 31 dispersion also increases evidently with increasing the LRD concentration, but no abrupt increase is detected as shown in Fig. 4b. The viscosity of the LRD/PR 31 dispersion is closely related to the stability of the three-dimensional colloidal network composed of hydrated LRD/PR 31 platelets. The more stable is the network, the higher is the viscosity. The main driving forces for forming the network of LRD/PR 31 are the "face-to-edge" electrostatic interaction between the positively charged "edge" and the negatively charged "face" of LRD/PR 31 platelets, and the hydrogen bonding and van der Waals forces among the functional groups surface.[37] Thus, the viscosity of the LRD/PR 31 dispersions should be mainly dependent on the concentration of LRD and the interactions between LRD and PR 31. The increase in viscosity of the LRD/PR 31 aqueous suspension may also contribute to the dispersing of PR 31. A critical viscosity of about 500 mPa·s is needed to disperse PR 31 very well in water, which is corresponding to a concentration 20 mg/mL of LRD in the LRD/PR 31 dispersion. Thus, sufficient LRD is necessary to fully modify PR 31 during solid-state grinding, and then disperses it well in water.

With a LRD concentration of 20 mg/mL, the concentration of PR 31 increases almost linearly from 0.55 to 9.97 mg/mL with increasing the dosage of PR 31 from 1 to 20 mg/mL (Fig. 4c). However, the percentage of PR 31 first increases quickly from 53.67% to 86.68% with increasing the PR 31 dosage from 1 to 4 mg/mL, and then decreases evidently to 49.66% with further increasing the PR 31 dosage to 20 mg/mL. The increase of the dosage of PR 31 also leads to an evident increase in viscosity of the LRD/PR 31 aqueous suspension as shown in Fig. 4d. This is attributed to the enhanced host-guest interaction between LRD and PR 31 with the increase of the dosage of PR 31.

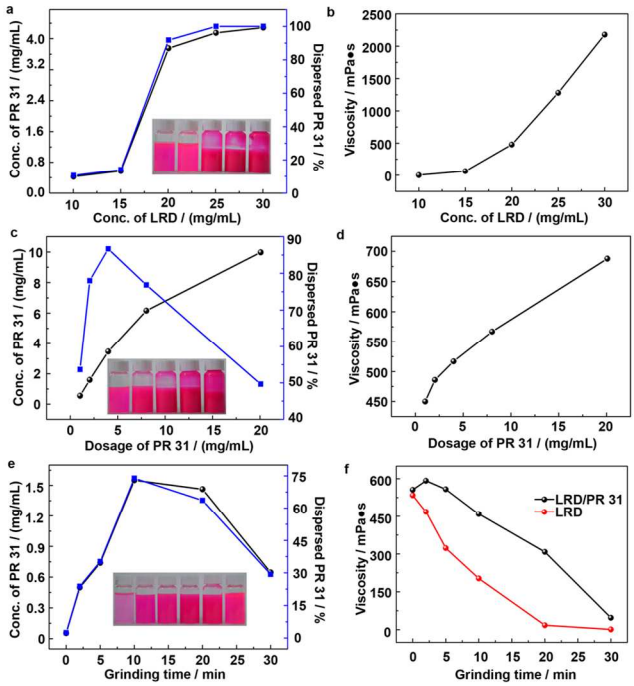

Fig. 4. Variation of concentration and percentage of dispersed PR 31 in aqueous suspensions with (a) concentration of LRD (4 mg/mL PR 31), (c) dosage of PR 31 (20 mg/mL LRD) and (e) grinding time (2 mg/mL PR 31, 20 mg/mL LRD), and variation of viscosity of (b) LRD/PR 31 dispersion with concentration of LRD (4 mg/mL PR 31), (d) LRD/PR 31 dispersion with dosage of PR 31 (20 mg/mL LRD) and (f) LRD/PR 31 and LRD aqueous suspensions with grinding time. The suspensions were obtained by ultrasonication for 30 min, and then centrifugation at 8000 rpm for 20 min.

Solid-state grinding is another important factor besides the concentration of LRD in dispersing PR 31. Without grinding, the concentration of PR 31 is only 0.05 mg/mL and less than 2.5% of PR 31 is dispersed in water (Fig. 4e). Two minutes of grinding obviously increases the concentration of PR 31 to 0.50 mg/mL. The concentration further increases to 1.55 mg/mL with increasing the grinding time to 10 min and approximately 75% of PR 31 is dispersed in water. Grinding could enhance the host-guest interaction between LRD and PR 31, and then transport PR 31 into aqueous phase. However, grinding time beyond 30 min induces a decline of the concentration of PR 31 to 0.65 mg/mL.

Intensive grinding for a long period of time exerts a destructive effect on the platelets of LRD, which is evidenced by a major recession of viscosity of the LRD/PR 31 aqueous suspension from 556 to 47.4 mPa·s after 30 min of grinding (Fig. 4f). This phenomenon further indicates that viscosity of the LRD/PR 31 suspension has a great influence on dispersibility of PR 31. It also can be seen from Fig. 4f that the viscosity of the LRD/PR 31 aqueous suspension is obviously higher than that of pristine LRD with the same grinding time, which further proves the host-guest interaction between LRD and PR 31 in the solid-state grinding process.

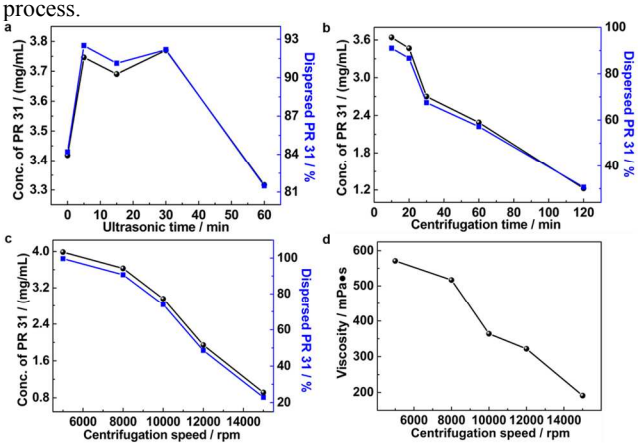

Fig. 5. Variation of concentration and percentage of dispersed PR 31 in aqueous suspension with (a) ultrasonication time, (b) centrifugation time (centrifugation at 8000 rpm) and (c) centrifugation speed (20 min of centrifugation), and (d) variation of viscosity of LRD/PR 31 with centrifugation speed (20 min of centrifugation). The mixture of 40 mg of PR 31 and 200 mg of LRD was ground for 10 min and then ultrasonicated and centrifugated.

It can be seen from Fig. S3 that the concentration and percentage of dispersed PR 31 decrease with increasing the amount of water due to the decrease of LRD concentration. LRD/PR 31 is highly hydrophilic and disperses very well (>84%) in water even without ultrasonication (Fig. 5a). Whereas ultrasonication could obviously improve the dispersibility of LRD/PR 31 in water (>90%) by disintegrating the agglomerated LRD/PR 31 formed during grinding. The percentage of dispersed PR 31 decreases to 81.50% with increasing the ultrasonication time to 60 min. Ultrasonication for a long period of time may also damage the platelets of LRD, similar to the case of long time grinding, which eventually depresses the dispersibility of PR 31. In spite of the lower concentration and percentage of dispersed PR 31 with increasing the centrifugation time and speed (Fig. 5b, c), the LRD/PR 31 suspensions still show excellent stability. The percentage of dispersed PR 31 is ~70% after centrifugation at 8000 rpm for 30 min (Fig. 5b) or at 10000 rpm for 20 min (Fig. 5c). The influence of 20 min of centrifugation at 5000 rpm on the concentration of PR 31 is negligible and almost 100% of PR 31 is dispersed (Fig. 5c). The viscosity of the LRD/PR 31 aqueous suspension decreases with increasing centrifugation speed (Fig. 5d). This is because more PR 31 is removed from the LRD/PR 31 aqueous suspension with increasing the centrifugation speed, which further confirmed the interaction between LRD and PR 31. In addition, no sediment can be observed after storage in ambient conditions for over 4 months.

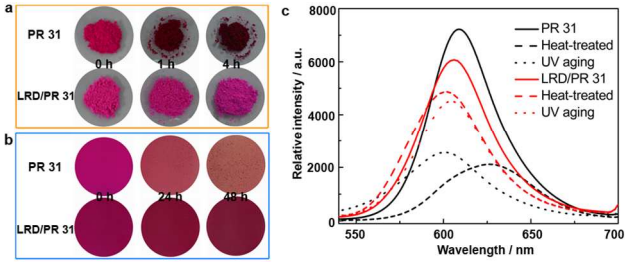

Fig. 6. Images of PR 31 and LRD/PR 31 after (a) thermal aging at 150°C for 4 h and (b) UV irradiation for 48 h, (c) variation of solid-state fluorescence spectra of PR 31 and LRD/PR 31 after thermal aging and UV irradiation.

Moreover, we have tried to use palygorskite, the most frequently used clay mineral for the preparation of Maya Blue pigments, instead of LRD to prepare water dispersible hybrid pigments via the same approach. However, the dispersibility of the palygorskite/PR 31 pigment is poor in water (Fig. S4). A clearly solid-liquid boundary can be seen at 40 mL for the palygorskite/PR 31 suspension after standing in ambient conditions for 24 h. By contrast, the LRD/PR 31 dispersion shows excellent stability and no sedimentation of the pigment can be observed.

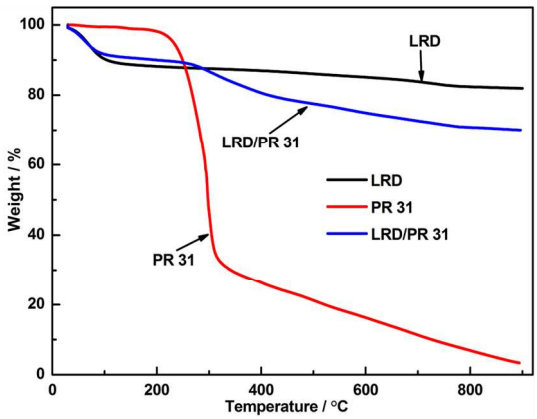

Fig.7. TGA curves for LRD, PR 31 and LRD/PR 31 in the range of 0 to 900 °C in N_2 atmosphere. The mixture of 40 mg of PR 31 and 200 mg of LRD was ground for 10 min.

Thermal stability and photostability of LRD/PR 31

The stability of LRD/PR 31 and PR 31 against thermal aging and UV irradiation is shown in Fig.6. The color of PR 31 changed significantly from bright rose-red to dark reddish brown after thermal aging at 150 °C for 4 h, whereas LRD/PR 31 remained bright rose-red and only slight color change was observed (Fig. 6a). The difference in thermal stability is more convincible from the fluorescence spectra of LRD/PR 31 and PR 31 (Fig. 6c). The fluorescence intensity of PR 31 decreases from 7223 to 2114 a.u. after thermal aging. In addition, an obvious bathochromic shift from 609 to 626 nm of the emission wavelength of PR 31 was observed indicating the chemical structure of PR 31 was changed. In contrast, the fluorescence intensity of LRD/PR 31 decreases from 6070 to 4866 a.u. after thermal aging, which is much better than that of pristine PR 31. The decomposition of LRD/PR 31 begins at 295 °C according to the TGA curves, which is much higher than that of pristine PR 31 (220 °C) (Fig. 7). Similar trends can also be observed from the UV irradiation tests. PR 31 became

light pink and the fluorescence intensity decreased to 2556 a.u. after UV irradiation, whereas no evident change in the colour and the fluorescence intensity was detected for LRD/PR 31 (Fig. 6b, c). Thus, the thermal and UV stability of PR 31 have been greatly enhanced after modified by LRD, which is due to the interactions between LRD and PR 31, and the shielding effect of LRD.[38, 39]

Conclusions

In summary, we fabricated water-dispersible stable LRD/HFOPs pigments via a simple grinding-ultrasonication procedure inspired by Maya Blue. The LRD/PR 31 aqueous suspension features high stability and a high PR 31 concentration (9.97 mg/mL). The concentration of LRD and hand-grinding play important roles in effectively dispersing PR 31. The interactions between host and guest involve van der Walls, π-π, electrostatic, hydrogen bonding between phenolic hydroxyl groups of PR 31 and silanols of LRD as well as dye-dye hydrophobic interactions. However, the exact interactions between LRD and PR 31 are not clear yet, and will be studied in further work. The interactions between PR 31 and LRD occur on the external surface of LRD and the entrance of the micropores of LRD, however, the PR 31 molecules cannot intercalate into the layers of LRD plates. Moreover, the thermal and UV stability of PR 31 are greatly enhanced by the host-guest interaction between LRD and PR 31 as well as the shielding effect of LRD. We believe that the new method may pave the way for the applications of HFOPs in various fields via a green aqueous approach.

Acknowledgements

The authors are grateful for financial support of the "Hundred Talents Program" of the Chinese Academy of Sciences, the open funding (CASXY2013-02) the Xuyi Center of Attapulgite Applied Technology Research Development & Industrialization of the Chinese Academy of Sciences, and the Key Technology R&D Program of Jiangsu (BE2014102).

Notes and references

[a] *Center of Eco*-material *and Green Chemistry, Lanzhou Institute of Chemical Physics, Chinese Academy of Sciences, Lanzhou, 730000, P. R. China. E-mail: jpzhang@licp.cas.cn, aqwang@licp.cas.cn*
[b] *Graduate University of the Chinese Academy of Sciences, 100049 Beijing, P. R. China.*
[c] *R&D Center of Xuyi Palygorskite Applied Technology, Lanzhou Institute of Chemical Physics, Chinese Academy of Science, Lanzhou 730000, China.*

† Electronic Supplementary Information (ESI) available: [standard curve, concentration of PR 31, zeta potentials of LRD suspensions, XRD patterns, digital images and video]. See DOI: 10.1039/b000000x/

1 P. Gregory, *High-technology applications of organic colorants*, Plenum Press, New York, 1991.
2 G. Chisholm, B. Hay, K. D. M. Harris, S. J. Kitchin and K. M. Morgan, *Dyes. Pigments*, 1999, **42**, 159.
3 B. Di Credico, G. Griffini, M. Levi and S. Turri, *ACS Appl. Mater. Inter.*, 2013, **5**, 6628.
4 R. Pardo, M. Zayat and D. Levy, *Chem. Soc. Rev.*, 2011, **40**, 672.
5 L. A. Mühlstein, J. Sauer and T. Bein, *Adv. Funct. Mater.*, 2009, **19**, 2027.
6 R. Li, C. S. Santos, T. B. Norsten, K. Morimitsu and C. Bohne, *Chem. Commun.*, 2010, **46**, 1941.
7 P. Bugnon, *Prog. Org. Coat.*, 1996, **29**, 39.
8 O. V. Makarova, A. E. Ostafin, H. Miyoshi, J. R. Norris and D. Meisel, *J. Phys. Chem. B*, 1999, **103**, 9080.
9 H. Berke, *Chem. Soc. Rev.*, 2007, **36**, 15.
10 S. Fantacci, A. Amat and A. Sgamellotti, *Accounts. Chem. Res.*, 2010, **43**, 802.
11 A. Domenech, M. T. Domenech-Carbo, C. Vidal-Lorenzo and M. L. Vazquez de Agredos-Pascual, *Angew. Chem. Int. Ed.*, 2012, **51**, 700.
12 H. Van Olphen, *Science*, 1966, **154**, 645.
13 A. Domenech, M. T. Domenech-Carbo and M. L. Vazquez de Agredos-Pascual, *Angew. Chem. Int. Ed.*, 2011, **50**, 5741.
14 P. Gómez-Romero and C. Sanchez, *New J. Chem.*, 2005, **29**, 57.
15 B. Hubbard, W. Kuang, A. Moser, G. A. Facey and C. Detellier, *Clay. Clay. Miner.*, 2003, **51**, 318.
16 E. Fois, A. Gamba and A. Tilocca, *Micropor. Mesopor. Mat*, 2003, **57**, 263.
17 G. Chiari, R. Giustetto and G. Ricchiardi, *Eur. J. Mineral.*, 2003, **15**, 21.
18 R. Giustetto, F. X. Llabrés i Xamena, G. Ricchiardi, S. Bordiga, A. Damin, R. Gobetto and M. R. Chierotti, *J. Phys. Chem. B*, 2005, **109**, 19360.
19 R. Giustetto, D. Levy and G. Chiari, *Eur. J. Mineral.*, 2006, **18**, 629.
20 A. Doménech, M. T. Doménech-Carbó, M. Sánchez del Río, M. L. Vázquez de Agredos Pascual and E. Lima, *New J. Chem.*, 2009, **33**, 2371.
21 C. Dejoie, E. Dooryhee, P. Martinetto, S. Blanc, P. Bordat, R. Brown, F. Porcher, M. S. Del Rio, P. Strobel and M. Anne, *arXiv preprint arXiv:1007.0818*, 2010.
22 L. A. Polette, G. Meitzner, M. Jose Yacaman and R. R. Chianelli, *Microchem. J.*, 2002, **71**, 167.
23 A. Tilocca and E. Fois, *J. Phys. Chem. C*, 2009, **113**, 8683.
24 M. S. del Río, E. Boccaleri, M. Milanesio, G. Croce, W. van Beek, C. Tsiantos, G. D. Chyssikos, V. Gionis, G. H. Kacandes and M. Suárez, *J. Mater. Sci.*, 2009, **44**, 5524.
25 E. Lima, A. Guzmán, M. Vera, J. L. Rivera and J. Fraissard, *J. Phys. Chem. C*, 2012, **116**, 4556.
26 C. Dejoie, P. Martinetto, N. Tamura, M. Kunz, F. Porcher, P. Bordat, R. Brown, E. Dooryhée, M. Anne and L. B. McCusker, *J. Phys. Chem. C*, 2014, **118**, 28032.
27 A. Dundigalla, S. Lin‐Gibson, V. Ferreiro, M. M. Malwitz and G. Schmidt, *Macromol. Rapid. Comm.*, 2005, **26**, 143.
28 J. Zhang and B. Li, *J. Mater. Chem. A*, 2013, **1**, 10626.
29 M. M. Lezhnina, T. Grewe, H. Stoehr and U. Kynast, *Angew. Chem. Int. Ed.*, 2012, **51**, 10652.
30 S. Deguchi, S.-a. Mukai, M. Tsudome and K. Horikoshi, *Adv. Mater.*, 2006, **18**, 729.
31 G. Koshkakaryan, L. M. Klivansky, D. Cao, M. Snauko, S. J. Teat, J. O. Struppe and Y. Liu, *J. Am. Chem. Soc.*, 2009, **131**, 2078.
32 T. Nicolai and S. Cocard, *Langmuir.*, 2000, **16**, 8189.
33 Q. Wang, J. L. Mynar, M. Yoshida, E. Lee, M. Lee, K. Okuro, K. Kinbara and T. Aida, *Nature*, 2010, **463**, 339.
34 Y. Liu, J. Xu, W. Wang and A. Wang, *J. Disper. Sci. Technol*, 2013, 130806063734003.
35 X. Liu and J. K. Thomas, *Langmuir.*, 1991, **7**, 2808.
36 V. Martínez Martínez, F. López Arbeloa, J. Banuelos Prieto, T. Arbeloa López and I. López Arbeloa, *Langmuir.*, 2004, **20**, 5709.
37 A. Shahin and Y. M. Joshi, *Langmuir.*, 2010, **26**, 4219.
38 M. Ghadiri, H. Hau, W. Chrzanowski, H. Agus and R. Rohanizadeh, *RSC Advances*, 2013, **3**, 20193.
39 R. R. Tiwari and U. Natarajan, *J. Appl. Polym. Sci.*, 2008, **110**, 2374.